Performance Studies of a NOvA 53 MHz RF Cavity

Frederic Jones

Stony Brook University

Supervised by

David Wildman

Fermilab National Accelerator Laboratory,

Batavia, IL 60510

May 23rd – August. 12th 2011

Table of Contents

1. ABSTRACT

Three new RF cavities are required to perform multi-batch slip stacking in the Recycler Ring to increase the proton intensity of the NuMI beamline for the NOvA project to study muon to electron neutron oscillations. Two RF cavities will operate at different frequencies, and one will be used as a spare. The cavities are made from high conductivity copper (OFHC) and operate in the quarter-wavelength transverse electromagnetic mode with a length slightly reduced by the gap capacitance at the accelerating voltage end. In this study, we present results from low power measurements of one of these cavities. We used coaxial cables hooked-up to a Network Analyzer to transmit power into its structure and measure the resonant modes. After adjusting the length of the cavity, the fundamental mode which is used to accelerate the beam during slip stacking was measured very close to the desire operational value of 52.809 MHz. The higher order modes of the cavity were also identified and prototype dampers were constructed to test their ability to suppress them. To determine the frequency tuning range of the cavity, tuners were also developed. These RF devices were able to optimize the cavity's performance.

2. INTRODUCTION

The Fermilab Recycler Ring (RR) will be converted to a pre-injector to the Main Injector (MI) for the NOvA (NuMI Off-Axis Electron Neutrino Appearance) project to study muon to electron neutrino oscillations. This improvement will reduce the MI's cycle time from 2 sec to 1.33 sec and increase the beam power, which is necessary to observe the ultra-rare neutrino oscillations. [1]

Multi-batch slip stacking is the method that will increase the proton intensity. This process is performed in the RR, and doubles the number of protons per batch injected from the Booster. Twelve Booster Batches will be slip stacked to yield the required beam intensity. Three new RF systems will be constructed for this purpose. Two of them will operate at a 1200 Hz difference in frequency; the third will be used as a spare.

In this study, we present results from low power measurements of a 52.809 MHz RF cavity that will used to perform multi-batch slip stacking in the RR. The cavity is a quarter-wavelength resonator that operates in the TEM (transverse electromagnetic) standing wave mode with a short at one end and an open at the other. The length of the cavity is slightly foreshortened by a capacitance at the open end, where 150 kV will be applied to accelerate the beam.

We constructed prototypes of the RF devices that will be used to optimize the cavity's performance during operation. HOM (Higher Order Mode) dampers and frequency tuners were developed and their effect on the resonant frequency was evaluated.

3. CHARACTERISTICS OF THE CAVITY

Figure 1 displays a solid model of the cavity. The concentric inner and outer conductors form a transmission line that is open at one end and short circuited at the other. At the open end, a capacitance was created to provide an accelerating voltage that is parallel to the beam axis. The length of the cavity is determined by the required resonant frequency and this gap capacitance. Radial coupling ports were made on the sides for frequency tuners, dampers and power couplers to be inserted.

The cavity's dimensions were adjusted so that a low R_{sh}/Q_0 value (~15Ω) is achieved which helps to prevent multi-bunch beam instabilities. The shunt impedance (R_{sh}) of the structure is the resistance that is presented to the beam current [2]. The strengths of the resonant modes can be characterized by this quantity. R_{sh} is a measure of the power losses and can be calculated using Equation 1, where V_{gap} is the accelerating voltage at the gap and P_D is the power dissipated, mainly in the cavity walls.

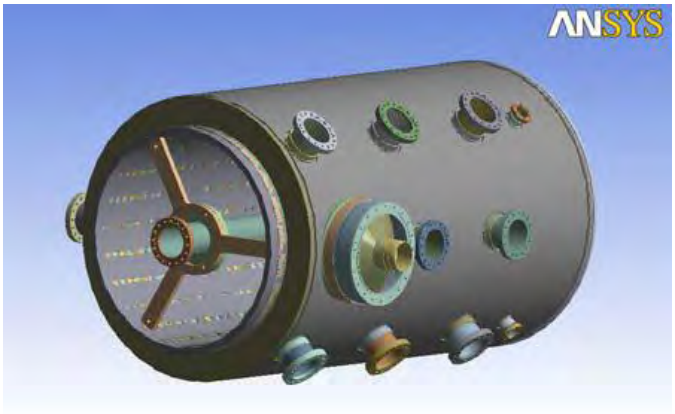

Figure 1. Solid model of the cavity

$$R_{sh} = \frac{V_{gap}^2}{2P_D} \qquad (1)$$

The peak voltage and maximum power that will be applied to this cavity during operation is 150kV and 150kW, respectively; therefore, the shunt impedance is 75kΩ. Q_0, which is the ratio of the stored energy to the energy dissipated, will be 5000 since the R_{sh}/Q_0, which is a geometrical factor that does not vary with power losses, will be ~15Ω. R_{sh}/Q_0 depends on the dimensions of the cavity; namely, the characteristic impedance, which is determined by the radius of the inner conductor,r_1, and outer conductor,r_2, as given in equation 2.

$$R_c = \frac{\ln(r_2/r_1)}{2\pi\varepsilon_0 c} = \frac{\pi R_{sh}}{4Q_0} \qquad (2)$$

The length of r_1 was adjusted to 13.5 inches and r_2 to 16 inches. Therefore, the value of R_c is 10.194Ω.

A schematic view of the cavity is displayed in Figure 2. The path between the concentric conductors forms a capacitance whose value is dependent upon distance between the walls. That is, on the values of r_1 andr_2. Transient beam loading instability can be reduced if there is a relatively high capacitance between these walls, which increases the energy storage capability of the cavity with respect to the beam. This is what creates the low R_{sh}/Q_0 value.

Using Equation 3 with the desired operational frequency of 52.809 MHz we found the length of the center conductor to be 55.91". This calculation, however, does not take into account the effect of the gap capacitance which reduces the length of the cavity. We can solve for the true value using equation 4, where $\frac{1}{\omega C_{gap}}$ is the reactance at the gap, $\beta = \frac{2\pi}{\lambda}$, and l is the center conductor's length

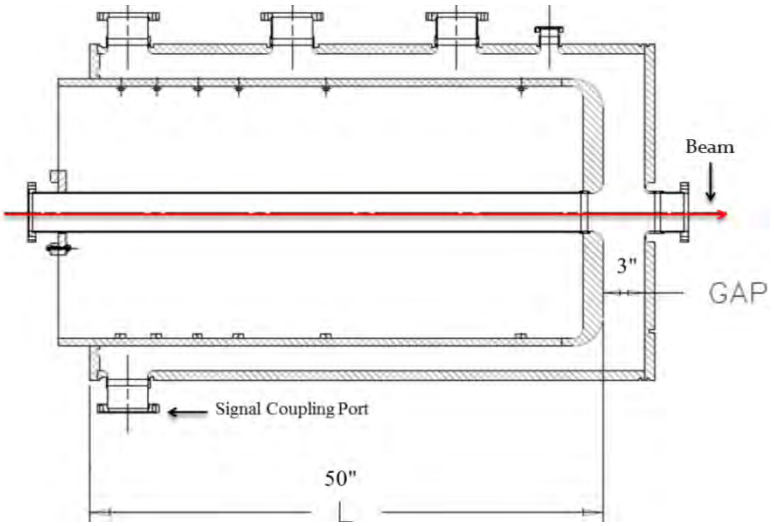

Figure 2. Schematic view of the cavity

$$c=\lambda f \tag{3}$$

$$R_c \tan \beta l = \frac{1}{\omega C_{gap}} \tag{4}$$

After performing the necessary calculations and adjustments to the gap length, we determined the correct value of the center conductor to be 50". The outer conductor's length is 60".

Since this cavity will be under high vacuum during operation, it is necessary to evaluate the effect of multipacting, which can reduce the accelerating voltage and degrade its performance. The multipactor effect occurs in a vacuum when electrons oscillate at a certain velocity between the cavity walls and produce secondary electrons when they impact the surface. Consequently, an avalanche of electrons could build-up which absorbs the RF power and endangers its ability to accelerate the beam. Multipacting starts at a specific threshold voltage (V_t) and has an upper limit (V_{um}) as given by Equations 5 and 6, respectively. We calculated V_t for this cavity to be 679.77V and V_{um} to be 1.26 kV. Since V_{gap} will be 150kV, it is safe to say that multipacting will not occur at the gap end. However, due to the varying electrical field in the cavity there is a possibility that it may develop at another location, which we can be determined using the voltage turns ratio. According to our calculations, multipacting will onset at 0.14" from the shorted end and stop at 0.26".

$$V_t = 0.039(fd)^2 \tag{5}$$

$$V_{um} < 1.85V_t \tag{6}$$

Fortunately, there is a reliable way to avoid multipacting; namely, by conditioning the cavity through exposure to high RF voltage, which cleans the inner surface and prevents the electron build-up process by lowering the secondary electron emission coefficient.

4. CAVITY TESTING

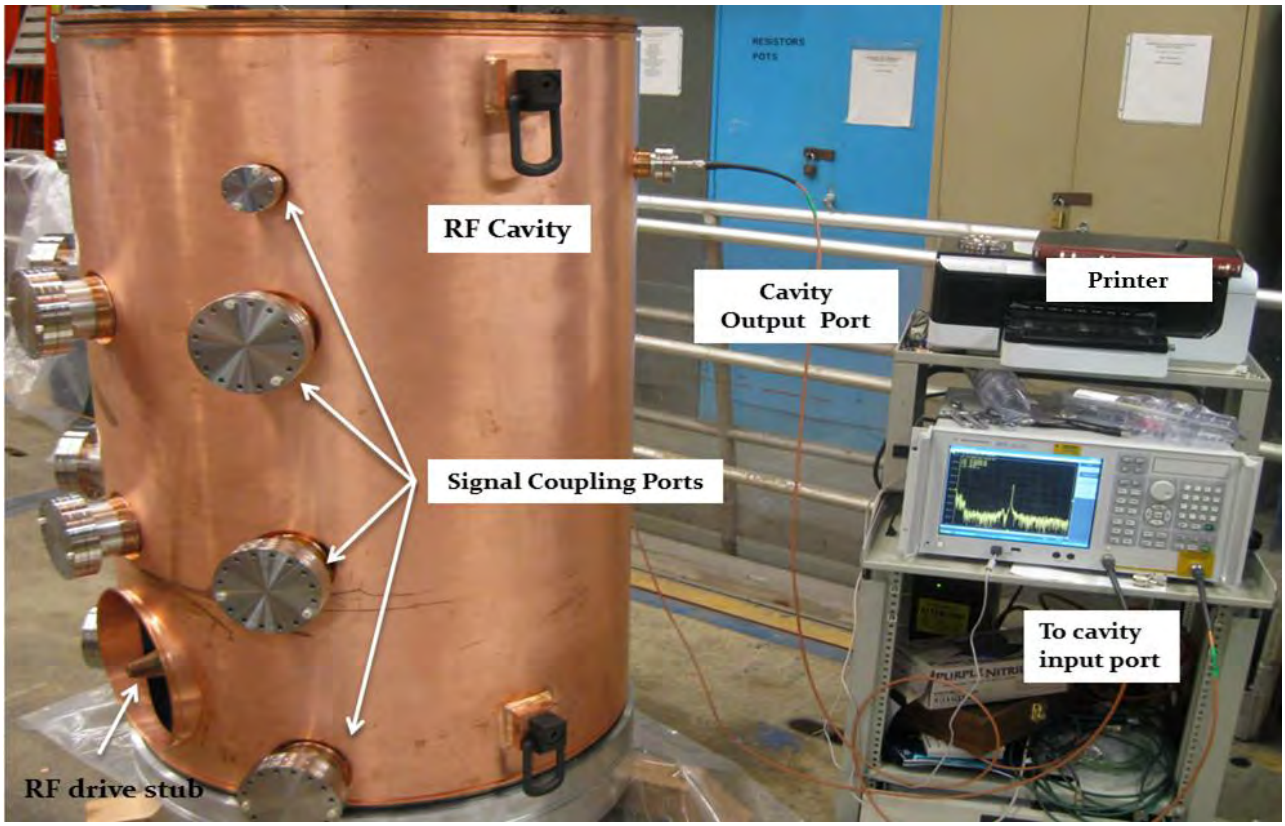

Figure 3. Measurement set-up of the RF Cavity.

We measured the frequency response of the cavity by transmitting an RF signal into its structure at its resonant frequency and picking-up the output returns. Figure 3 displays the measurement set-up, where one can see the RF cavity and signal coupling ports, which are not only used to couple RF power into and out of the cavity but also for attaching RF devices such as tuners and HOM dampers which are useful for optimizing its performance. Also shown in the figure is the Network Analyzer (NA) that is used to weakly excite the cavity fields and detect the output responses. Measurements were taken using field probes that are mechanically connected to RG 58 coaxial transmission lines which are hooked-up to the NA. The field probes were connected to the cavity via the signal coupling ports and extended into the gap between the inner and outer conductors. Transmission (S_{21}) responses was measured from 0-1GHz.

4.1 FREQUENCY DEPENEDENCE ON GAP SPACING

Using the measurement set-up of Figure 3, we were able to determine a very important relationship, which is the dependence of the resonant frequency on the gap spacing between the center conductor and the end plate of the outer conductor. The cavity is adjusted so that it is resonated by the gap capacitance as given in equation 4. By lowering this capacitance via adjusting the fixture at the shorted end of the cavity and increasing the gap spacing, we can increase the resonant frequency, and vice-versa. This allows us to establish the required operational value. Figure 5 displays the results from changing the gap length and measuring the resonant frequency of the cavity. The gap length that gave us the required frequency was 3 inches.

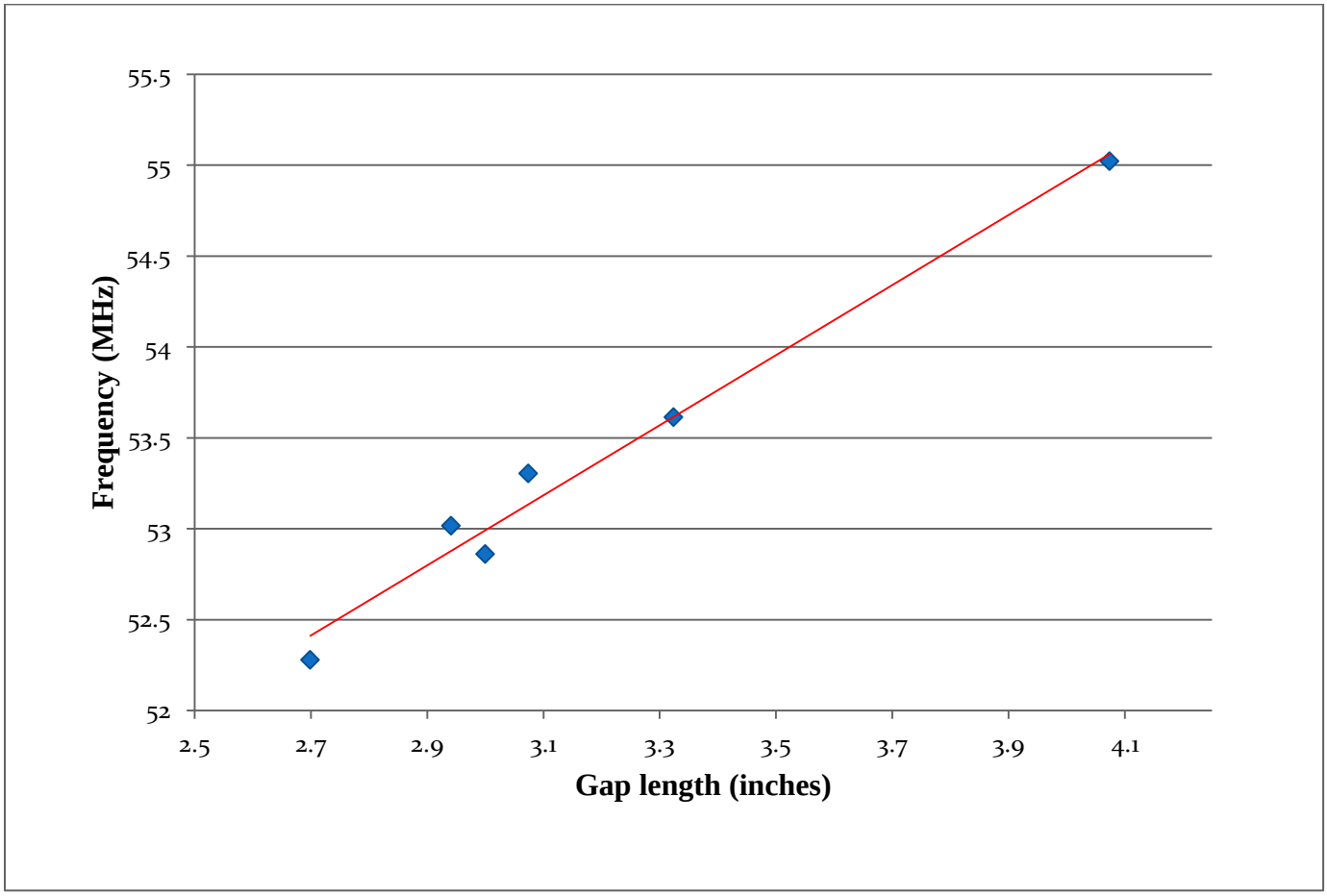

Figure 4. Resonant frequency dependence on the gap distance.

4.2 THE EFFECT OF HOMs

Higher order modes (HOMs) are resonant modes of the cavity that have frequencies much larger than the fundamental mode which is used to accelerate the beam. There are two types of HOMs in this cavity: TEM modes, which have the electric and magnetic fields perpendicular to the direction of beam propagation, and TM modes, which only have the magnetic field transverse to the beam path. These frequencies can affect the cavity's performance in several ways: by inducing beam losses and coupled bunch instabilities. The latter is caused when the wakefield, which is a field set-up by the beam when it traverses the cavity, of one particle bunch affects the following bunch. HOMs resonate at the frequencies of the wakefields, which can lead to exponential growth of the beam instability and correspondingly, degradation of the cavity's performance.

For proper operation, it is necessary to identify the HOMs and subsequently damp them. Furthermore, it is important to distinguish the HOMs so that we can locate the harmonics ones (TEM), which are the most significant.

4.2.1 FREQUENCY SPECTRUM OF THE CAVITY

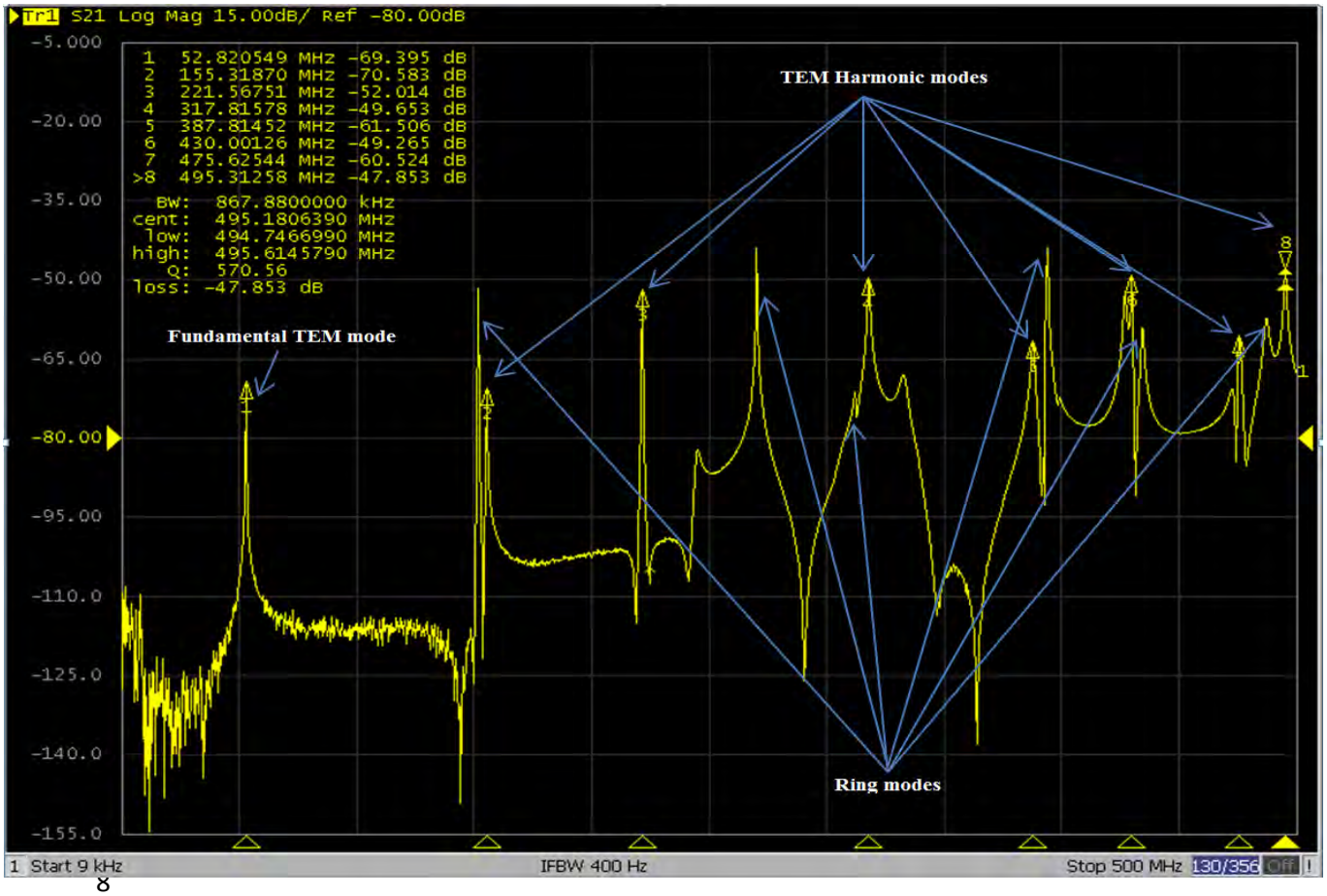

Figure 5. Frequency Spectrum of the Cavity. HOMs are identified from 0-500MHz. The Fundamental mode is shown on the far left.

Table 1. TEM MODES FROM 0-500MHz

TEM mode		
Measured(MHz)	Calculated(MHz)	Type of mode
52.853577	52.809	Fundamental
155.10314	158.427	1st harmonic
221.70607	264.045	2nd harmonic
318.01453		
387.74436	369.663	3rd Harmonic
429.95748		
475.29751 494.99696	475.281	4th Harmonic

Table 2. RING MODES FROM 0-500MHz

Measured (MHz)	Calculated (MHz)	Type of Ring mode
151. 66356	141.0	λg/4, m=1
	221.0	3λg/4, m=1
270.17299	261.9	λg/4, m=2
312.07341	312.5	3λg/4, m=2
394.31085	327.1 387.0 394.7	5λg/4, m=1 λg/4, m=3 5λg/4, m=2
486.86703	422.9 422.9 440.7 486.8 492.8	3λg/4, m=3 3λg/4, m=3 7λg/4, m=1 5λg/4, m=3 7λg/4, m=2

We used a power pick-up coupler to distinguish the HOMs of the cavity. This device is a rigid 50Ω coaxial line that has a circular loop at its end which couples to the fields inside of the cavity. Since the TEM and ring modes have different oscillation paths, we can identify them by

rotating the loop at different axial positions with respect to the direction of the B fields. If the normal of the loop is along the direction of the B-field, the TEM modes will be picked-up. Conversely, if we orient it perpendicular to this orientation, the TM modes will be detected. Figure 4 displays the spectrum of the cavity from 0-500 MHz with the HOMs identified using the power-pick-up coupler. Table 1 and 2 is a record of the TEM and Ring modes from 0-500MHz, respectively.

5. GAP VOLTAGE MONITOR

Under loaded conditions, when the peak operational voltage (150KV) is across the gap, power measurements can become potentially dangerous due to the high voltages that will be induced on the monitor. Therefore, it is necessary to modify the field probes to a gap voltage monitor whose location inside of the vacuum housing should be such that it detects low voltage fields. The side monitor should produce a 1:100000 voltage ratio between the gap voltage. That is, we would like to see 1.5 V on the monitor when 150kV is across the gap.

The side monitor is a field probe that has a 1 inch diameter circular plate at its end, which forms a capacitance with the center conductor of the cavity. The detected voltage is dependent on how far the probe extends into its vacuum housing. The vacuum housing, a $\frac{3}{2}\lambda$" diameter tube, acts like a waveguide beyond cutoff attenuating the fields from the cavity to the monitor's plate. We can calculate λ_{cutoff} for the monitor using equation 7, where r is the radius of the plate.

$$\lambda_{\text{cutoff}} = \frac{2\pi r}{2.405} \tag{7}$$

At a resonant frequency of 52.809 MHz ($\lambda \approx 6$ m), the cavity fields are well beyond λ_{cutoff} which is 2.16" for this monitor. We can determine the attenuation achieved using the following equation.

$$-\frac{54.7dB}{\lambda_{\text{cutoff}}}\sqrt{1-(\lambda_{\text{cutoff}}/\lambda)\text{^}2} \;\approx\; -\frac{54.7dB}{\lambda_{\text{cutoff}}} = -25.32 \text{ dB} \tag{8}$$

Figure 6 displays the gap voltage monitor, where L is the extension into the vacuum housing. After adjusting this length, we determined the required value that would yield the 1:100000 monitor to gap voltage ratio to be 0.85". We implemented a commercial N type 2.75" CF feed-through with a L of 0.8845" to test the effectiveness of the measurement scheme. The attenuation calculated from equation 8 using this distance is -43.44 dB since the depth of the vacuum housing is 2.6".

We used an Agilent high impedance probe (model 85024A) to calibrate the losses in the coaxial lines so that we can determine an accurate value for Vgap. The transmitted power into the cavity from the Network Analyzer is measured in dB. We used equation 9 to determine the output power (P_{out}) after 1mW input power (P_{in}) were transmitted into the cavity. This allowed us to determine Vgap.

$$dB = 10 \log \frac{P_{out}}{P_{in}} \quad (9)$$

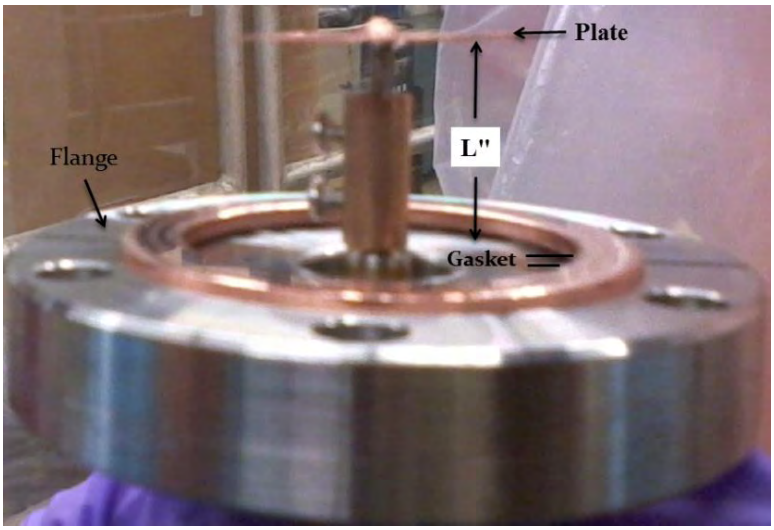

Figure 6. Gap voltage monitor. L is the extension into the vacuum housing in inches.

Vgap was determined to be 0.3773 V without power amplifier and 8.1419V with the amplifier. Table 1 summarizes the results.

Table 3. Measurements of a commercial N type 2.75" CF feed-through

Effective length (inches)	Power loss (db)	$V_{monitor}$ (μV)	V_{gap} (V)	$V_{monitor}/V_{gap}$ ($\times 10^{-5}$)	configuration
0.8075	-71.15	94.08	8.1419	1.156	w/o gasket
0.8845	-70.53	87.60		1.076	w gasket

(Appendix 3 contains the measurements of the prototype monitor that was used to determine the effective length, L)

6. HOM DAMPER

The gap voltage monitor previously analyzed can be used to construct an HOM damper. An HOM damper is a device that is used to suppress the detrimental HOMs. It is a quarter-wavelength coaxial transmission line that resonates at the frequency of the HOM. An effective damper should attenuate the shunt impedance of these modes, which determines their relative strengths, without degrading the fundamental mode. We can observe the effectiveness of the damper by measuring the power losses of the HOM modes using the Network Analyzer.

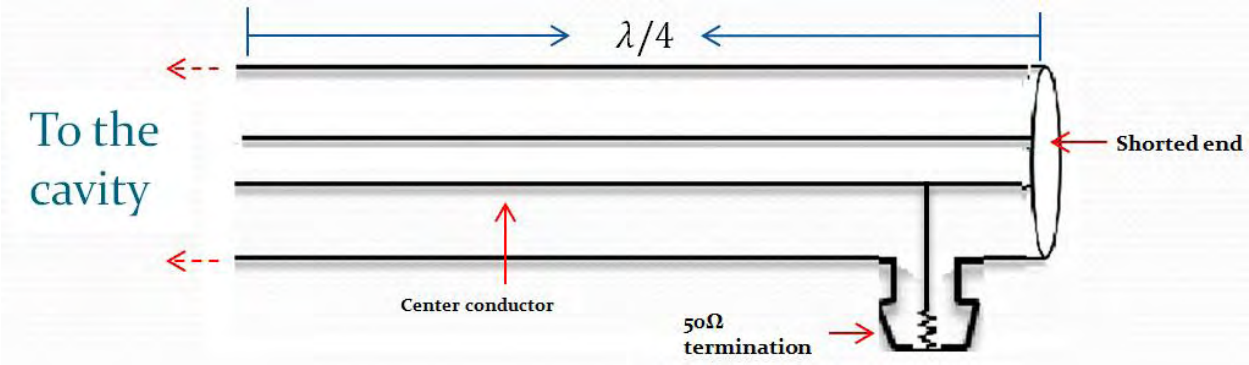

Figure 7. Schematic view of a HOM damper.

Figure 7 displays a schematic view of the damper, which is short-circuited at one end and connected to the cavity at the other. At a certain location on its structure, a 50Ω termination is placed to absorb the transmitted RF power, which can be determined using the following set of equations, where d is the length of the damper ,N is the voltage turns ratio, R is the 50 Ω termination and R_{sh} is the shunt impedance. (Note that the shunt impedance is calculated using equation 2).

$$x = \mathrm{d} \times \frac{\sin^{-1}(\mathrm{N})}{90^{\circ}} \tag{10}$$

$$\mathrm{N} = \sqrt{\frac{\mathrm{R}}{\mathrm{R_{sh}}}} \tag{11}$$

Two prototype dampers were created, one for the 151 MHz ring mode and 221 MHz TEM mode. A 50Ω RG-58 polyethylene coaxial transmission line was used for both frequencies. The length of the 221 MHz and 151 MHz damper was adjusted to 10" and to 11.3125", respectively. The measured Q-value for the former was 21.674 and 17.29 for the latter. We calculated the optimal location for the 50Ω termination to be 1.22" from the shorted end for the 221 MHz mode and 1.55" for the 151 MHz mode. However, due to limited fine adjustability of the electrical connectors, we placed the termination at 1.4" from the shorted end for both. The results for these dampers are shown in figure 8.

Before Damping

After Damping

151MHZ Ring Mode dB loss -53

dB loss -75

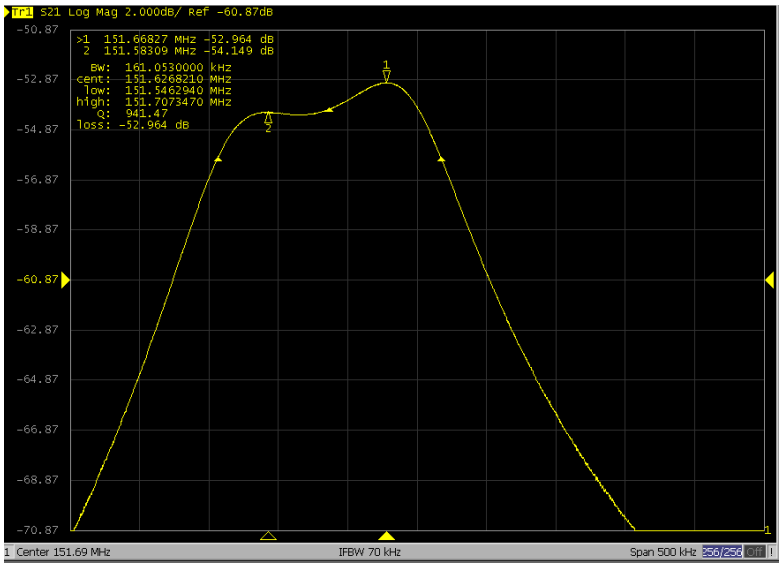

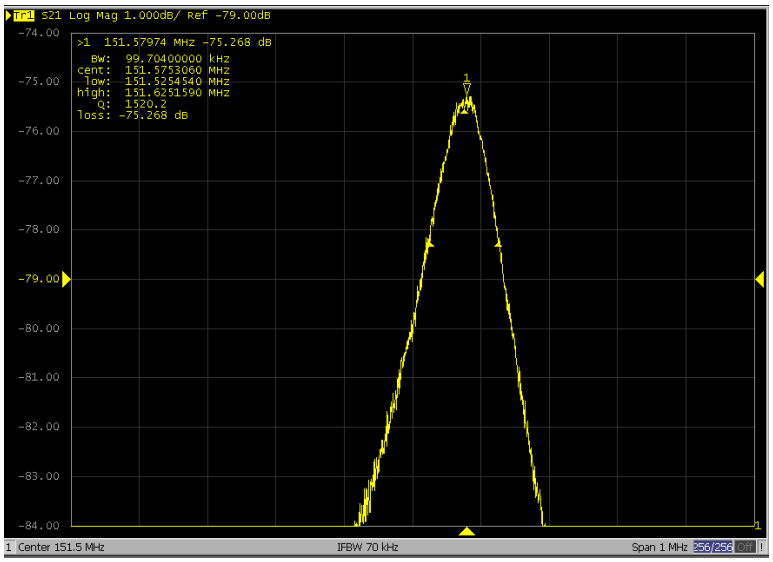

221MHZ TEM Mode dB loss -54

dB loss -66

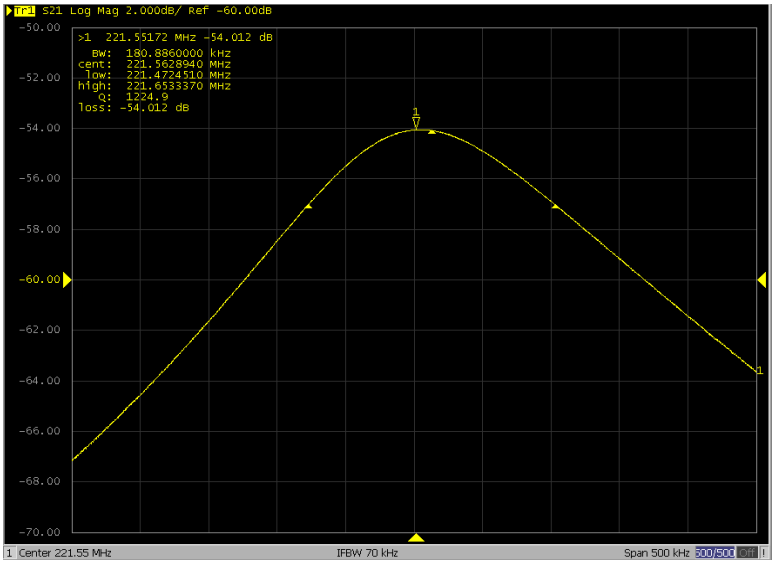

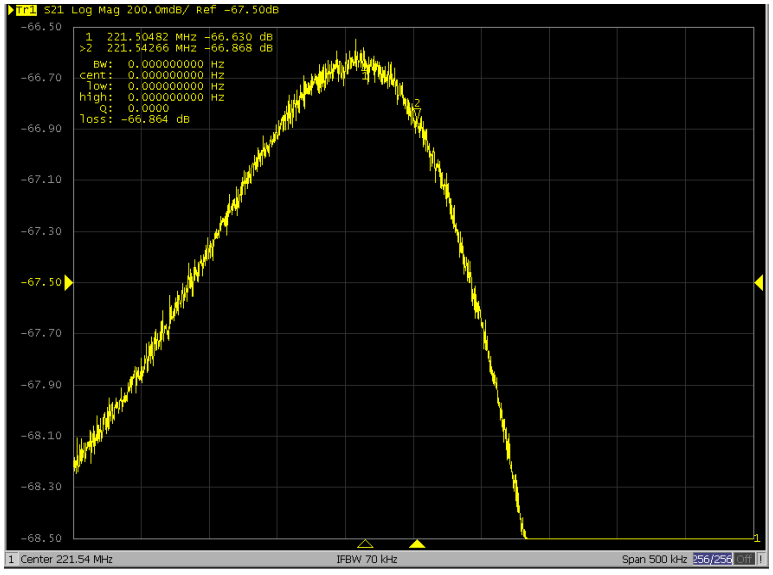

Figure 8. Before and after damping of the 151 MHz ring mode and 221 MHz TEM mode

7. CAVITY TUNERS

The resonant frequency is dependent on the cavity's geometry, which can be altered by environmental conditions such as temperature and pressure. In order to maintain a correct phase relation with the beam (so that it is properly accelerated), it is necessary to adjust the frequency when changes occur. A reliable way of doing this is with frequency tuners.

Two RF Tuners will be used to adjust the cavity's resonant frequency during operation. One is a fast garnet tuner loaded with aluminum doped ferrite and the other is a mechanical tuner that alters the frequency by changing the effective volume of the cavity. Prototypes of these devices were created to test the effectiveness of the proposed tuning scheme.

7.1 ALUMINUM DOPED FERRITE LOADED GARNET TUNER

An aluminum- doped yittrium iron garnet (YIG) tuner will be used for fast tuning of the resonant frequency under loaded conditions. The tuner is a half-wavelength resonator that is inductively coupled to the cavity at one end and contains a perpendicularly biased ferrite stack at the other. By changing the bias field, the permeability of the ferrite will change, which in turn alters the current in the coupling loop inside the cavity. Correspondingly, the magnetic field content surrounding the coupling loop will changed, and as result, the resonant frequency of the cavity as well. [4]

Figure 9 displays a schematic view of the cavity with the aluminum doped YIG tuner. The bias field will have a bandwidth ~20kHz, which is essential to compensate for fast changes in beam loading.

The tuner can be modeled as transmission line whose effective length is dependent on the permeability of the ferrite [4].Therefore, cavity-tuner system can be represented by a parallel RLC circuit as shown in figure 10, where L_1, C_1, L_2, C_2 are the equivalent inductance and capacitance of the cavity and tuner, respectively, and M is the mutual inductance.

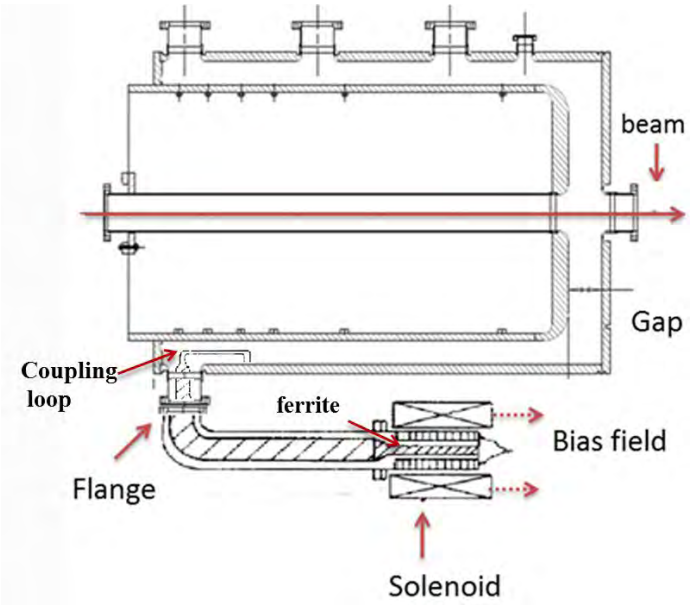

Figure 9. Cross-sectional view of cavity-tuner system

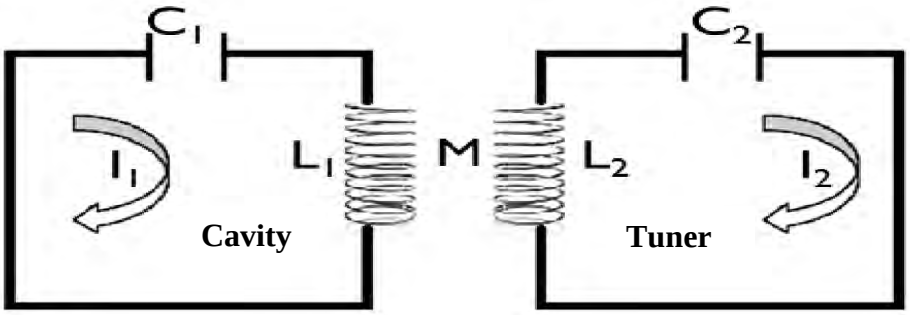

Figure 10. Equivalent circuit of the cavity-tuner system

The resonant frequency of the cavity with the tuner can be calculated as follows.

$$f_0 = \frac{1}{2\pi\sqrt{L_{eff}\, C_1}} \tag{12}$$

Where,

$$L_{eff} = L_1\left(1 - \frac{\frac{M^2}{L_1 L_2}}{1+\frac{Z_t}{Z_2}}\right) \tag{13}$$

Here Z_t is the impedance of the shorted transmission line and Z_2 is the reactance of L_1.

A prototype of the garnet tuner was constructed to measure the tuning range of the cavity. The tuner is a half-wavelength rigid coaxial waveguide that is loop coupled to the cavity at the open end and mechanically controlled at the shorted end. We adjusted the electrical length using elbow connectors. By changing the amount of adapters connected to the coaxial waveguide, we can alter the resonant frequency of the cavity. This is similar to how the permeability of the ferrite changes the effective length of the garnet tuner. We minimized the power losses in the prototype by substituting RG 58 cables with rigid coaxial waveguides of different lengths to establish an adequate tuning range. Figure 11, displays the prototype tuner. Note that the waveguides are connected at the indicated location to create a half-wavelength resonator.

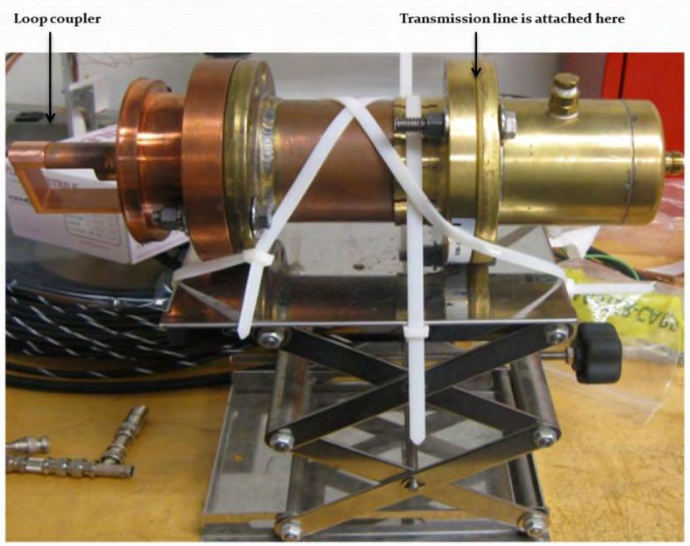

Figure 11. Rigid coaxial waveguide with loop coupler at its end. The coaxial waveguide that is used to create a half-wavelength resonator is not shown.

7.1.1 RESULTS OF PROTOTYPE GARNET TUNER

We performed transmission (S21) measurements of the cavity-tuner system. The electrical length of the tuner was determined using S11 measurements, where the length is observed in equivalent phase. We varied this distance by adjusting the number of elbow connectors attached to the end of the coaxial waveguide. The resonant frequency and Q of the system was measured at each position. A plot of the Frequency and Q versus the equivalent phase is shown in Figure 12. A tuning range ~ 20 kHz was observed, which is sufficient for proper operation.

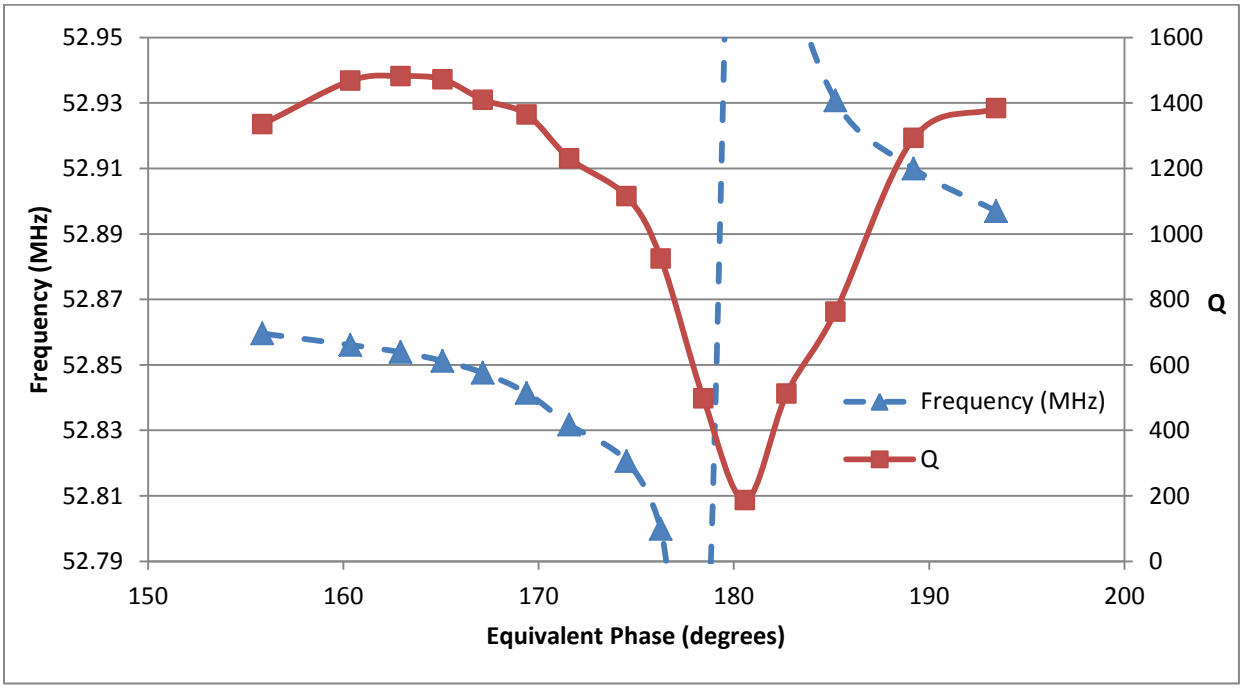

Figure 12. Resonant Frequency and Q as a function of the effective length of the prototype tuner measured in equivalent phase.

7.2 MECHANICAL TUNER

As previously stated, the resonant frequency of the cavity is dependent on its effective volume. Therefore, cavity tuning can be performed via perturbation techniques. According to Slater's theorem [5], an object inserted into the cavity removes a portion of its volume and alters the resonant frequency by an amount dependent on the square of the electric and magnetic field strengths at that location. If the object is introduced at a location where the B-field is at a maximum relative to the E-field, then the frequency will shift positively, and vice-versa. The perturbed frequency can be calculated as follows.

$$\omega^2 = \omega_o^2 \left(1 + k \frac{\int_{\Delta\tau} (\mu H^2 - \varepsilon E^2)\, d\tau}{\int_V (\mu H^2 + \varepsilon E^2) dv} \right)$$

(10)

Where ω_0 is the unperturbed frequency, ω is the perturbed frequency, dv is the volume displaced by the object in the cavity, $d\tau$ is the volume of the object, H is magnetic field, and E is the electric field.

Using this principle, a mechanical tuner was implemented to measure the frequency tuning range of the cavity. The tuner is a cylindrical copper block whose effect on the frequency depends on its location and depth inside the cavity. The latter is changed by an externally operated adjuster. The tuner is shown in Figure 13, where the flange is used for connection to cavity's port.

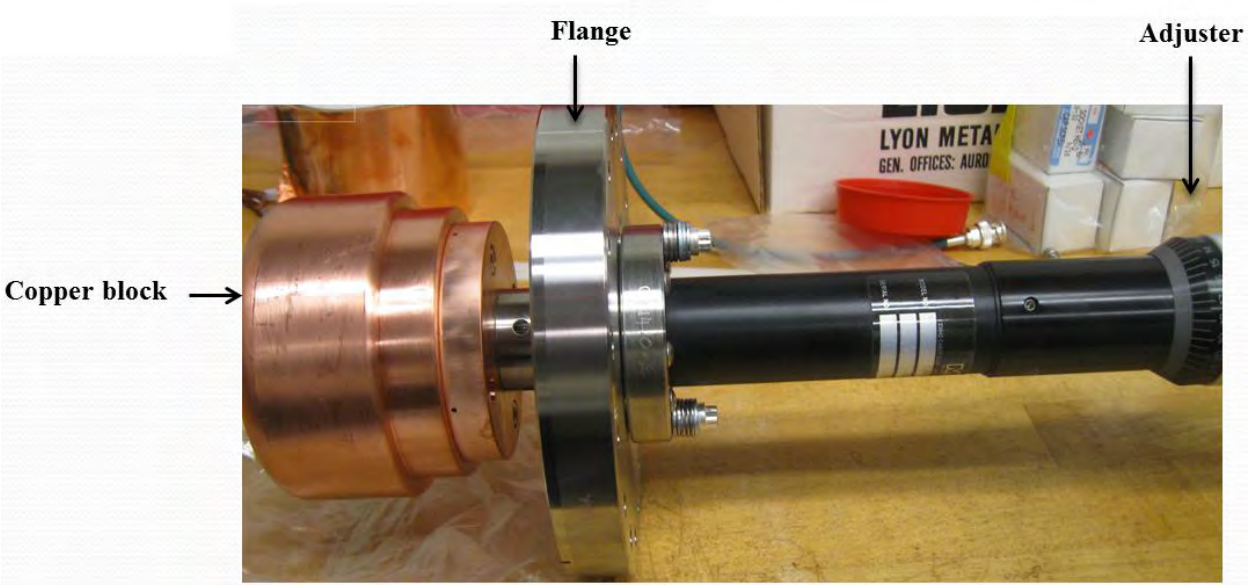

Figure 13. Mechanical tuner

7.2.1 RESULTS OF MECHANICAL TUNER

Transmission (S21) responses were measured at different locations and depth inside the cavity for the mechanical tuner. When the block was placed at the gap end where the electric strength is large and the magnetic field strength is small, the resonant frequency decreased according to slater's theorem. On the other hand, at the shorted end, the frequency increased due the presence of relatively strong magnetic fields. The results are shown in figure 14.

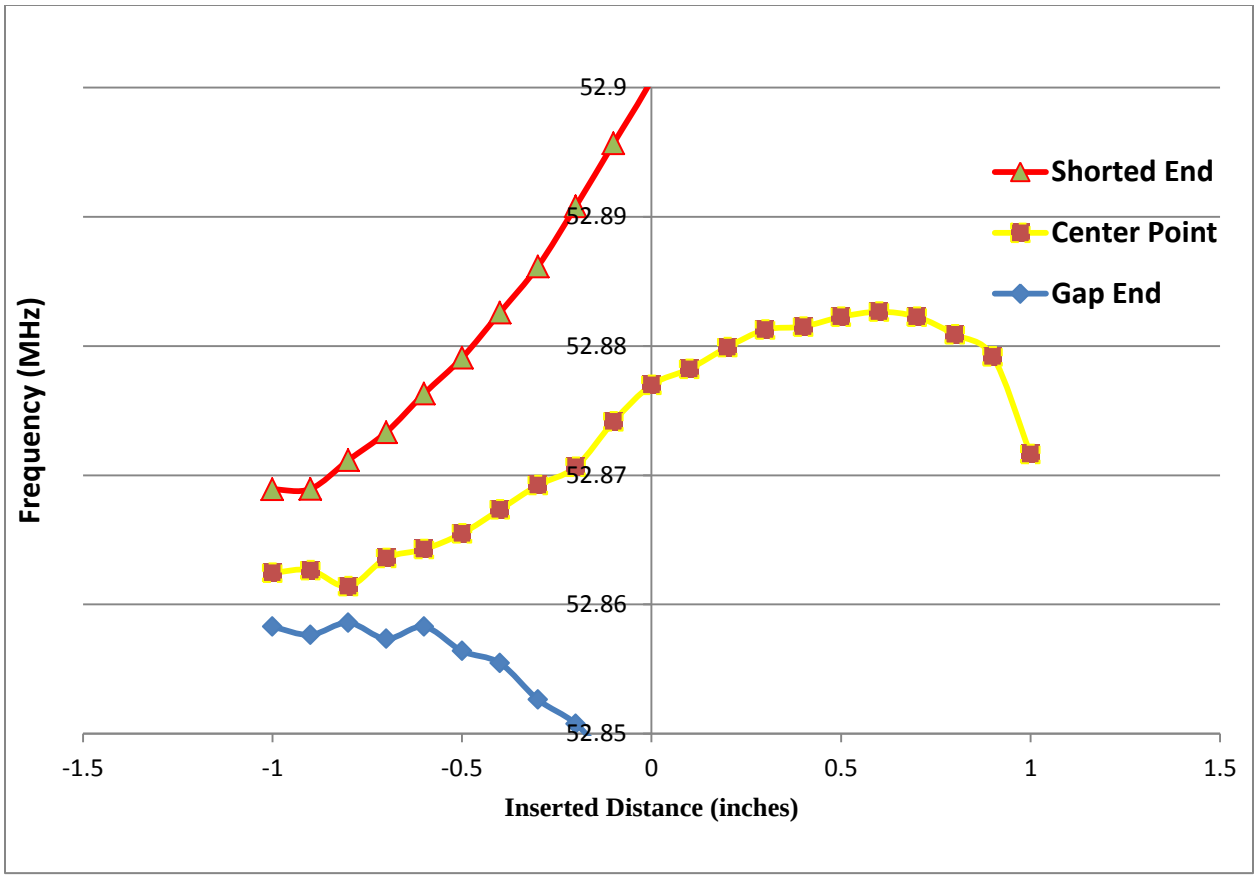

Figure 14. Change in the resonant frequency as a function of the mechanical tuner's depth and location inside of the cavity.

8. CONCLUSION

The resonant Frequency of the cavity was adjusted very close of the desired operational value of 52.809MHz. All HOM modes were identified. The Prototype HOM dampers and Tuners developed in this study proved to be successful in optimizing the cavity's performance. Namely, the damper reduced the strengths of the 151 and 221 MHz modes, which verifies the effectiveness of the proposed damping scheme. The fast cavity-tuner system demonstrated the necessary 10 kHz tuning range that is required to reliably adjust the resonant frequency.

9. ACKNOWLEDGEMENTS

I would thank my supervisors David Wildman and Robyn Madrak for their patience and guidance throughout this work. Special thanks goes to Jamieson Olsen, Dianne Engram, Dr. James Davenport, Linda Diepholz and the rest of the SIST committee for giving me this tremendous opportunity and for making it a rewarding experience.

10. REFERENCES

[1] K. Seiya, et al, "Progress in Multi-batch Slip stacking in the Fermilab Main Injector and Future Plans," Proceedings of the 23rd Particle Accelerator Conference, May 4th – 8th, 2009, Vancouver, British Columbia, Canada.

[2] J.E. Griffin, "A Numerical Example of an RF Accelerating System", in R.A. Carrigan, F.R.Huson, and M. Month, ed., *Physics of High Energy Particle Accelerators (Fermilab Summer School, 1981),* American Institute of Physics, New York, 1982, p. 564-582.

[3] H. Elnaiem, "Prototype NOvA RF Cavity for the Fermilab Recycler Ring," May 18th-August 7th, 2009, internal publication.

[4] S.M. Hanna, "YIG Tuners For RF Cavities," IEEE Transactions on Magnetics, vol.28, NO.5, September 1992.

[5] L.C. Maier, Jr. and J.C. Slater, "Field Strength Measurements in Resonant Cavities," Journal of Applies Physics, vol. 23, no. 1, pp. 68-77, January 1952.

APPENDIX 1

Table 4. Frequency dependence on inductive short.

Frequency (MHz)	
With short	**Without short**
61.01256	52.96088
153.62047	151.75536
221.48392	155.43257
244.37962	221.62242
282.15298	245.15659
312.62182	270.40679
328.54646	317.96543
349.86097	332.67428
391.50019	387.83249
428.37500	394.24265
434.00000	436.86304
478.75000	430.02314
489.62500	434.50844
500.25000	475.61789
525.12500	487.33333
534.12500	495.20325
552.87500	521.09569
561.85000	532.87930
566.26000	550.45028
576.25000	565.90056
605.95000	567.25141
621.79000	601.02251
632.59000	620.69418
642.76000	629.13696
668.77000	642.56098
692.89000	645.60038
710.68750	668.52871
715.75000	692.43902
719.31250	714.82927
726.53125	718.92683
769.65625	764.58537
789.15625	791.64853
816.90625	819.72983
831.62500	917.32708
878.06250	975.06066
894.55938	995.28705
916.84063	
977.35938	
994.68125	
996.55000	

20 Note that this will be used to short-circuit the spare cavity that will be installed in the Recycler Ring. This is done to prevent it from taking away energy from the beam.

APPENDIX 2

Table 5. Frequency comparison before and after welding the bottom fixture of the cavity.

Before Welding: Gap length= 3 inches	**After Welding:** Gap length+ two washers =3.218 inches
Frequency (MHz)	Frequency (MHz)
52.820549	52.87849
151.88127	151.35087
155.31870	155.72852
221.56751	220.76800
270.31663	246.72126
317.81578	269.86939
387.81452	309.25922
430.00126	317.07646
434.37618	330.69418
475.62544	386.75422
487.18773	392.72045
495.31258	426.26642
521.11695	472.08255
532.85178	485.81614
550.48781	519.27455
565.87242	550.22889
567.37336	558.61914
601.06942	587.66229
620.73171	627.03190
628.91182	644.78049
642.64540	668.01501
645.57223	693.50844
673.96811	716.74296
692.46404	727.22327
714.79049	749.68105
718.83990	762.02627
764.58724	770.69418
769.18387	814.42777
771.26329	875.23452
815.25954	897.82364
819.74672	913.99625
878.08005	923.69606
879.94059	940.46279
893.18324	991.81363
917.37023	
975.04690	
995.29393	

APPENDIX 3

Table 6. Measurements of the Prototype Side Monitor

Effective Length (inches)	Power loss (dB)	$V_{monitor}$ (μV)	V_{gap} (V)	$V_{monitor}/V_{gap}$ ($\times 10^{-5}$)
2.08	-69.3	108.39	0.3773	28.729
1.999	-71.15	87.60		23.217
1.86	-74.8	57.54		15.252
1.66	-79.7	32.73		8.676
1.39	-85.95	15.94		4.225
0.965	-95.5	5.31		1.407
0.895	-96.3	4.84		1.283
0.888	-97.1	4.42		1.117
0.85	-98.2	3.89		1.003

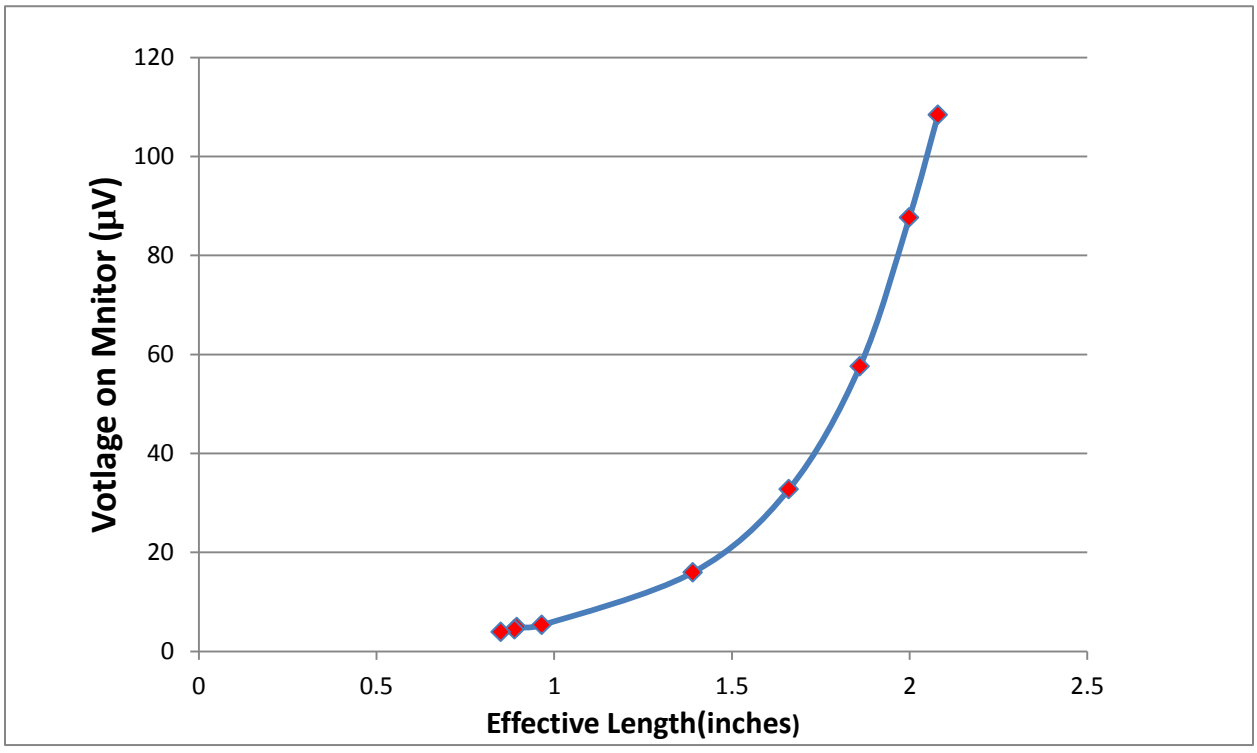

Figure 15. Dependence of the voltage on the effective length of the side monitor.

APPENDIX 4

Table 7. Change in the resonant frequency as a function of the mechanical tuner's Location and Depth inside of the RF Cavity.

MECHANICAL TUNER MEASUREMENTS

	Frequency (MHz)			**Q**		
Insertion Distance(inches)	Gap End	Middle	Shorted End	Gap End	Middle	Shorted End
-1	52.8582	52.8624	52.8689	1224	1180	1103
-0.9	52.8576	52.8626	52.8689	1270	1128	1219
-0.8	52.8586	52.8614	52.8712	1290	1154	1403
-0.7	52.8573	52.8635	52.87333	1315	1085	1380
-0.6	52.8583	52.8642	52.8763	1104	1113	1370
-0.5	52.8564	52.8655	52.8791	1004	1134	1339
-0.4	52.8555	52.8673	52.8826	1093	1130	1275
-0.3	52.8527	52.8692	52.8862	1131	1160	1181
-0.2	52.8508	52.8706	52.8908	1083	1163	1225
-0.1	52.8476	52.8742	52.8957	1133	1178	1192
0	52.8451	52.8769	52.9006	1144	1145	1000
0.1	52.8401	52.8782	52.9067	1173	1085	1090
0.2	52.8342	52.8799	52.9137	1215	1152	1179
0.3	52.8300	52.8812	52.9202	1165	1156	1098
0.4	52.8211	52.8815	52.9275	1143	1066	1109
0.5	52.8123	52.8822	52.9346	1110	1182	1200
0.6	52.8036	52.8826	52.9416	1150	1090	1092
0.7	52.7907	52.8822	52.9501	1142	1142	1232
0.8	52.7769	52.8808	52.9579	1189	1150	1215
0.9	52.7604	52.8792	52.9649	1206	1123	1038
1	52.7411	52.8716	52.97189	1130	1113	1254

APPENDIX 5

Figure 16. Prototype HOM Damper for the 155 MHz TEM modes

155 MHz TEM mode

Before Damping **dB loss -76.930**

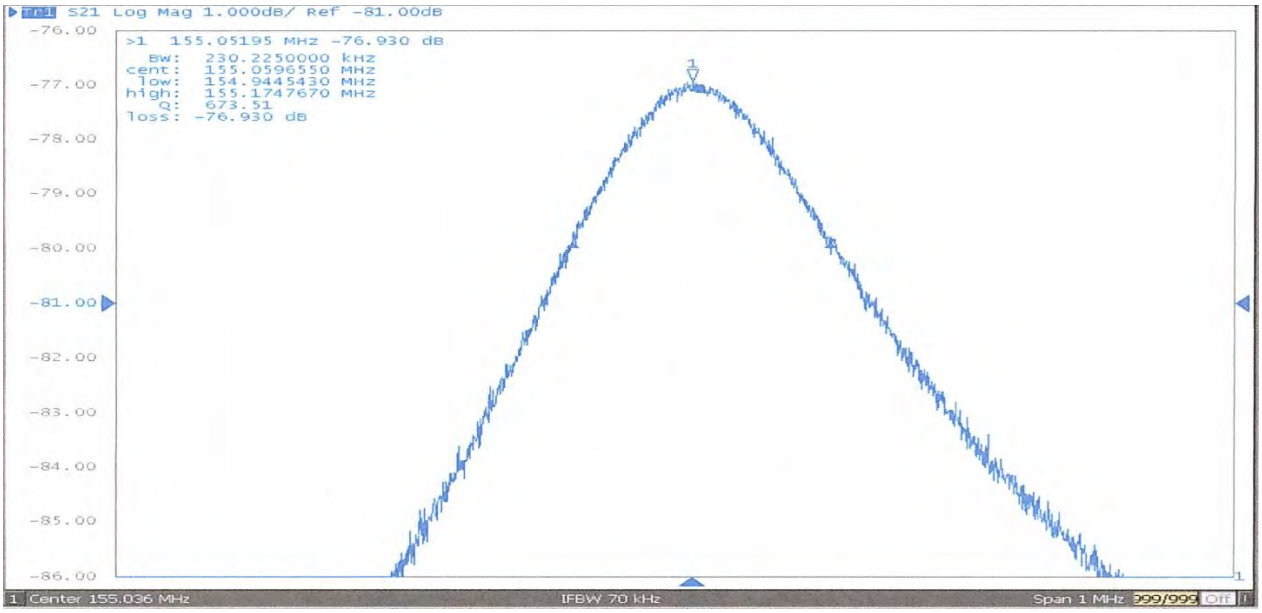

After Damping -Effective Length: 4 bullets, 4 barrels, a short and N type feed through, and 2 inches of wire. **dB loss -85.87**

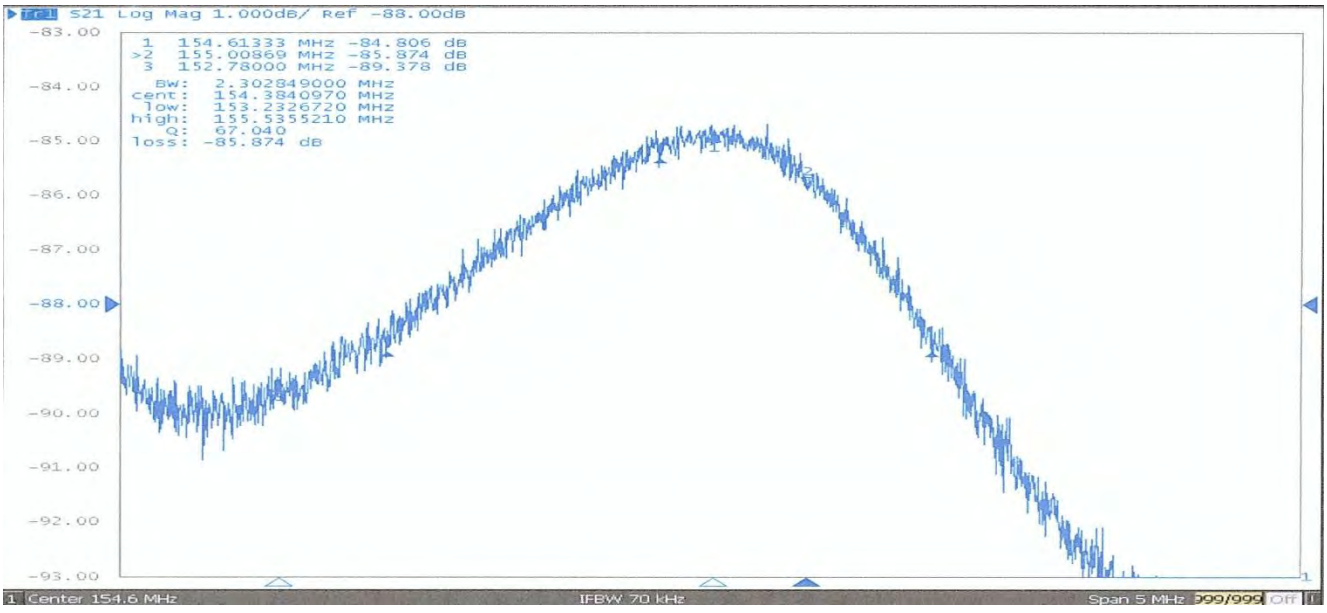

APPENDIX 6

Figure 17. The Effect of the 151/221 MHz Damper on the Resonant Frequency

No Damper **Frequency= 52.876957 MHz**

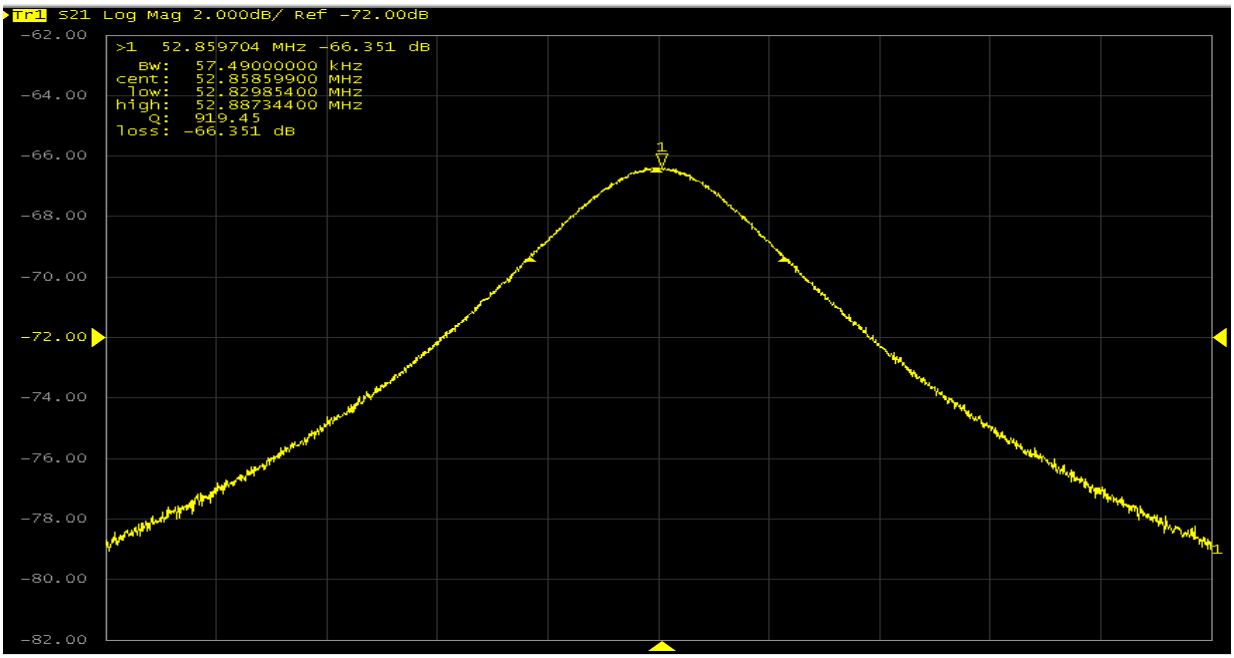

With Damper Connected **Frequency= 52.622892 MHz**

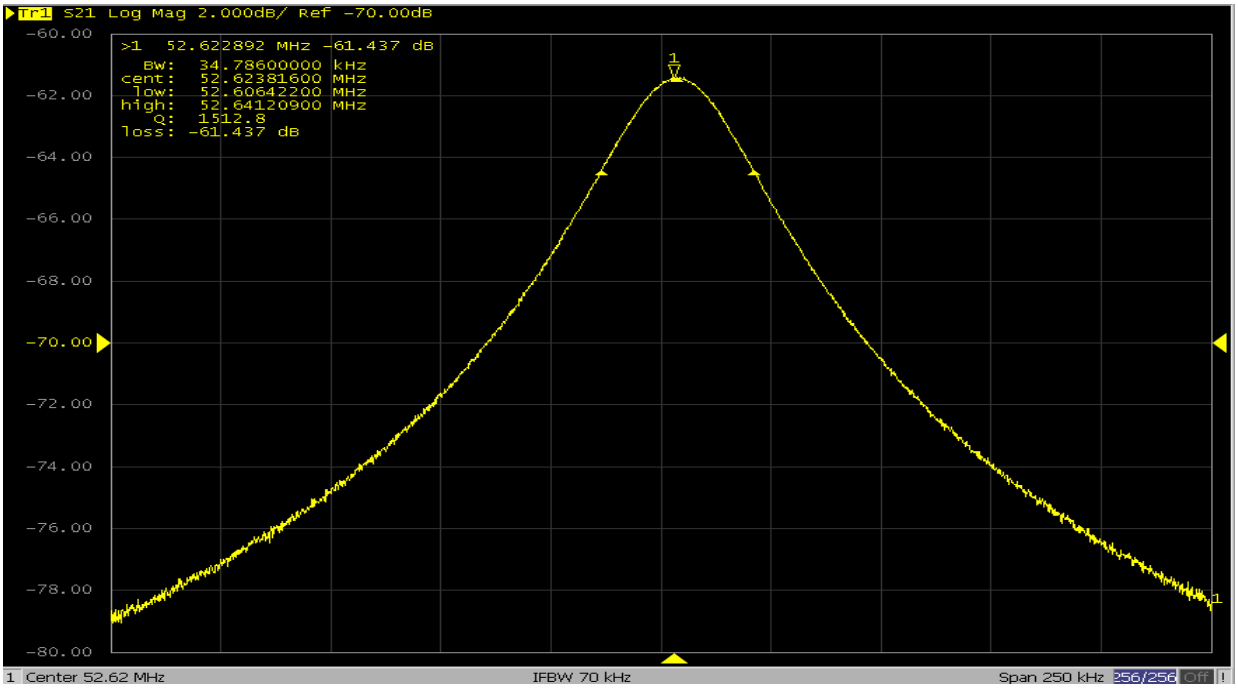

APPENDIX 7

Table 8. Frequency Dependence on Gap Length

Gap length (inches**)**	**Frequency** (MHZ)
4.074	55.021
3.324	53.613
3.074	53.304
3	52.861
2.941	53.017
2.699	52.278

APPENDIX 7

Table 9. Frequency change as a function of the equivalent phase of the rigid coaxial waveguide tuner.

# of adapters removed	Equivalent phase	Frequency (MHz)	Q
0	193.4395	52.89695	1384
2	189.2095	52.909965	1293
4	185.2045	52.93075	763
5	182.7045	52.98089	512
6	180.5795	53.14464	187
7	178.4395	52.7384	498
8	176.2645	52.79987	925
9	174.5045	52.8206	1115
10	171.5745	52.83175	1231
11	169.3995	52.841395	1365
12	167.1495	52.847575	1410
13	165.0945	52.851195	1472
14	162.9345	52.853897	1482
15	160.3695	52.856085	1468
17	155.8595	52.859575	1335